A Biodegradable Polycationic Paint that Kills Bacteria *In Vitro* and *In Vivo*

Jiaul Hoque, Padma Akkapeddi, Chandardhish Ghosh, Divakara S. S. M. Uppu and Jayanta Haldar*

Chemical Biology and Medicinal Chemistry Laboratory, New Chemistry Unit, Jawaharlal Nehru Centre for Advanced Scientific Research, Jakkur, Bengaluru 560064, India
E-mail: jayanta@jncasr.ac.in

Abstract: Bacterial colonization and subsequent formation of biofilms onto surfaces of medical devices and implants is a major source of nosocomial infections. Most antibacterial coatings to combat infections are either metal-based or non-degradable polymer-based and hence limited by their non-degradability and unpredictable toxicity. Moreover, to combat infections effectively, the coatings are required to display simultaneous antibacterial and antibiofilm activity. Herein we report biocompatible and biodegradable coatings based on organo-soluble quaternary chitin polymers which were immobilized non-covalently onto surfaces as bactericidal paint. The polycationic paint was found to be active against both drug-sensitive and drug-resistant bacteria such as methicillin-resistant *Staphylococcus aureus* (MRSA), vancomycin-resistant *Enterococcus faecium* (VRE) and beta lactam-resistant *Klebsiella pneumoniae*. The cationic polymers were shown to interact with the negatively charged bacterial cell membrane and disrupt the membrane-integrity thereby causing leakage of intracellular constituents and cell death upon contact. Importantly, surfaces coated with the polymers inhibited formation of biofilms against both Gram-positive *S. aureus* and Gram-negative *E. coli*, two of the most clinically important bacteria that form biofilm. Surfaces coated with the polymers displayed negligible toxicity against human erythrocytes and embryo kidney cells. Notably, the polymers were shown to be susceptible towards lysozyme. Further, subcutaneous implantation of polymer discs in rats led to 15-20% degradation in 4 weeks thereby displaying their biodegradability. In a murine model of subcutaneous infection, polymer-coated medical grade catheter reduced MRSA burden by 3.7 log

compared to non-coated catheter. Further, no biofilm development was observed on the coated catheters under *in vivo* conditions. The polycationic materials thus developed herein represent novel class of safe and effective coating agents for the prevention of device-associated infections.

Keywords: Biodegradable bactericidal paint, anti-infective biomaterials, drug-resistant bacteria, biofilm inhibition, organo-soluble quaternary chitin derivatives

1. INTRODUCTION

Over the last few decades usage of medical devices and implants such as catheters, contact lenses, cardiac pacemakers, hip implants, etc. has been increased to restore the function to damaged or diseased human organ tissue. However, the application of such biomaterials involves challenges, in particular, implant-associated infections resulting from the bacterial contamination and subsequent formation of biofilms.[1,2] It is estimated that almost 80% of the implant-related infections are associated with the biofilm formation.[3,4] Biofilms, protected by exo-polysaccharide (EPS) layer, are inherently immune towards the host-defense systems. Moreover, conventional antibiotic therapies, though helpful for mitigating systemic infections, are shown to be ineffective against biofilms.[5] Unfortunately, lack of appropriate treatments often necessitates removal of the contaminated implants and currently is the only viable option to eliminate implant-associated infections.[6] It is therefore crucial to avert bacterial colonization on the biomaterials surfaces to prevent infections. Coating of biomaterial surfaces with an effective antibacterial agent has been considered as a promising approach to thwart the microbial infections as the method does not alter the material's bulk properties.[7-13]

Bactericidal coatings developed by impregnating antibiotics, metal nanoparticles or various biocides are limited due to cumulative toxicity, increased development of microbial resistance and unwanted release of biocides.[14-18] Contact-active antibacterial coatings

developed by immobilizing antibacterial agents, e.g., antibacterial polymers, do not leach out from the surface and are less likely to allow bacterial resistance development.[19-24] However, covalent immobilization of antibacterial polymers on surfaces is limited due to several synthetic steps, using of harsh reagents and elevated temperatures.[25] To overcome these limitations, cationic antibacterial polymers that are insoluble in water and soluble in organic solvents have been developed and coated non-covalently onto surfaces in the form of paint.[26-30] The non-covalent modification of surfaces is thus simple, facile and easy to apply. However, the polymers used are mostly not biodegradable and often lack biocompatibility. The long-term exposure of non-degradable coatings might results in unpredictable cytotoxicity and hinders implant-tissue integration for many indwelling devices applications.[31-33] Moreover, for combating infections effectively the coatings are simultaneously required to inactivate bacteria and inhibit biofilm formation.[34,35] Thus an antibacterial coating should kill bacteria and prevent microbial colonization on medical devices or implants for desired period of time and disappear after its intended use. Herein, we report biodegradable and biocompatible paint developed from naturally occurring polymer chitin and demonstrate its use as safe antibacterial and antibiofilm coatings.

Chitin, the second most abundant polymer in nature, is used as wound dressings, artificial skin, preservatives in cosmetics, antithrombic and hemostatic materials, contact lenses, sutures and materials to support bone growth in orthopedic applications, etc.[36] In addition, it is inherently antimicrobial and susceptible towards human enzymes lysozymes thus making it completely biodegradable in human body.[37] However, insolubility of chitin in almost all the common organic solvents limits its practical use. Further, the antibacterial activity of pristine chitin is very low. The direct usage of chitin as antibacterial paint is thus limited due to its processability and lack of antibacterial activity. We envisioned that by introducing cationic charge and hydrophobicity into chitin and by balancing the

charge/hydrophobic ratio, water insoluble and organo-soluble polymers with degradable backbone and enhanced antibacterial activity could be developed. Moreover, as bacterial cell membrane is negatively charged due to the presence of anionic phospholipids, introduction of positive charges and hydrophobicity would render cationic chitin derivatives antibacterial. Here we, therefore, describe the design and synthesis of organo-soluble quaternary chitin polymers and demonstrate their use as biodegradable bactericidal paint. We systematically evaluated the effect of degree of quaternization (DQ) and length of hydrophobic alkyl chain on the material's solubility and antibacterial activity. The polycationic materials were able to kill both drug-sensitive and drug-resistant bacteria and inhibit biofilm formation upon painting onto various surfaces. Moreover, the polymers were shown to be non-toxic towards mammalian cells and susceptible towards hydrolytic enzymes under both *in vitro* and *in vivo* conditions. Interestingly, polymer coated catheter surfaces were shown to be effective in reducing bacterial burden and inhibiting biofilm formation *in vivo* in murine model thereby indicated the potential of the polymers to be used as paint in biomedical applications.

2. RESULTS AND DISCUSSIONS

2.1 Synthesis of Polymers. The water insoluble and organo-soluble polymers were synthesized by tosylation of chitin (degree of acetylation, DA ~75%) and subsequent quaternization of the tosylchitin (Scheme 1). Chitin was first selectively tosylated at the C-6 position of the sugar unit by reacting with tosylchloride (20 equivalents per sugar unit) at low temperature (8 ˚C).[38] Reaction at low temperature allowed the regioselective tosylation only at the primary hydroxyl group of the sugar unit of chitin. Three different tosylchitins were prepared as Tsch 1, Tsch 2, and Tsch 3 (obtained after 24 h, 48 h and 72 h of tosylation). As the degree of acetylation of chitin was ~75%, the remaining 25% free amine groups may interfere in the subsequent quaternization reactions of tosyl-chitin with *N,N*-dimethylalkylamines (e.g., via cross linking of polymer chains) (Scheme 1). The tosylchitins

were therefore reacted with acetic anhydride to protect the free amino group. Since the *N*-acetylation led to some *O*-acetylation, tosylchitin was further treated with methanolic KOH to remove the unwanted *O*-acetylation. It should be mentioned that during KOH treatment some detosylation also happened. The final *N*-acetylated tosylchitins were characterized by FT IR, ^{1}H NMR and elemental analysis (Supporting Information). The degree of substitution (DS) by tosyl group was calculated by sulfur to nitrogen (S/N) ratio (Table S1).[38] The tosylchitins were then finally reacted with *N,N*-dimethylalkylamines to synthesize various quaternized chitin derivatives (Scheme 1). Nine different quaternary polymers were prepared: **1a-1c**, **2a-2c** and **3a-3c** by reacting Tsch 1 (DS ~39%), Tsch 2 (DS ~48%) and Tsch 3 (DS ~55%) with *N,N*-dimethyl dodecylamine, *N,N*-dimethyl tetradecylamine, and *N,N*-dimethyl hexadecylamine respectively at 120 ˚C for 72 h (Scheme 1 and Table S2). The quaternary polymers were characterized by FT IR, ^{1}H NMR, and elemental analysis (Figure S1-S10, Supporting Information).

The quaternization of tosylchitins with *N,N*-dimethylalkylamines was confirmed from ^{1}H NMR as the NMR spectra clearly revealed the presence of only two doublet aromatic peaks at δ ~7.1 and ~7.5 ppm corresponding to protons of benzene ring in tosylate anion of quaternized chitin derivatives. By this method, for the first time, it was possible to synthesize completely water-insoluble quaternary chitin derivatives. The molecular weights of the organo-soluble polymers were determined by gel permeation chromatography (GPC) using pullulan as standard. The range of weight-average molecular weight (M_w) of the polymers was found to be 1.05×10^5 to 2.17×10^5 Da depending on the degree of quaternization and length of the alkyl chain (Table S3). The M_w of the polymers was found to increase with increase in both alkyl chain length as well increase in DQ (polydispersity index, PDI = 1.25-1.64). Solubility in water was tested by suspending the polymers in water, centrifuging the insoluble polymers after vigorous mixing followed by freeze drying the supernatant and

recording NMR with the dried samples. If no detectable signals were observed in the NMR spectra of the freeze dried samples the polymers were considered as water insoluble (within the detection limits of NMR). All the polymers except **1a** (**1b-1c**, **2a-2c**, and **3a-3c**) were found to be insoluble in water. The polymer **1a** (with $-C_{12}H_{25}$ long chain and 39% of degree of quaternization, DQ) was found to be slightly soluble in water (no further experiment was therefore performed with **1a**). However, all the polymers were found to be highly soluble in various organic solvents such as methanol, DMF, DMSO, etc. (Table S4).

2.2. Antibacterial Activity. To establish the simplicity of the coating procedure, polystyrene plates, glass slides or cover glasses were coated using the solution of polymers in methanol by simple brush-or dip- or spin-coating or drop-casting. After preparing the polymeric film in the polystyrene plate, antibacterial efficacy of the coatings was determined by adding bacterial suspensions in nutrient broth. The activity, expressed as minimum inhibitory amount (MIA), i.e., the minimum amount required to inhibit the growth of bacteria, was represented as the amount required/unit surface area. The cationic polymers were found to inhibit the growth of both Gram-positive *S. aureus* and Gram-negative *E. coli* completely as observed by visual turbidity (Table 1). The polymers showed different activity depending on the length of alkyl chain and the degree of quaternization (DQ). Among all the polymers, **1c** (with $-C_{16}H_{33}$ long chain and DQ of 39%) and **2c** (with $-C_{16}H_{33}$ long chain and DQ of 48%) were found to be most active polymers. MIA values of **1c** and **2c** were 0.06 μg/mm^2 and 0.12 μg/mm^2 against *S. aureus* and 3.9 μg/mm^2 each against *E. coli* (Table 1). Interestingly, activity for the polymers with DQ 39% and 48% was found to increase with increase in alkyl chain length against Gram-positive *S. aureus* and remained almost unchanged against Gram-negative *E. coli* upon increasing chain length (Table 1). For example, MIA values of **2a**, **2b**, and **2c** having $-C_{12}H_{25}$, $-C_{14}H_{29}$ and $-C_{16}H_{39}$ long chain and DQ of 48% were 0.48 μg/mm^2, 0.24 μg/mm^2 and 0.06 μg/mm^2 against *S. aureus* whereas MIA values of **2a**, **2b**, and **2c** were

7.8 μg/mm^2, 3.9 μg/mm^2 and 3.9 μg/mm^2 against *E. coli*. Antibacterial activity of the polymers with 55% DQ (**3a**, **3b** and **3c** having $-C_{12}H_{25}$, $-C_{14}H_{29}$ and $-C_{16}H_{39}$ long chain) was found to increase with increase in chain length against *S. aureus* (MIA values **3a**, **3b** and **3c** against *S. aureus* were 0.24 μg/mm^2, 0.24 μg/mm^2 and 0.12 μg/mm^2 respectively). However, the activity of **3a**, **3b** and **3c** was found to decrease with the increase in chain length against *E. coli* (MIA values **3a**, **3b** and **3c** were 15.6 μg/mm^2, 15.6 μg/mm^2 and 31.2 μg/mm^2 against *E. coli*) (Table 1). The polymers also showed activity against *P. aeruginosa*, an opportunistic bacterium known to cause many nosocomial infections. The most active polymer **2c** showed and MIA of 7.8 μg/mm^2 against *P. aeruginosa*. Not only against drug-sensitive bacteria, surfaces coated with the polymers showed activity against various drug-resistant bacteria such as methicillin-resistant *S. aureus* (MRSA), vancomycin-resistant *E. faecium* (VRE), and beta-lactam-resistant *K. pneumoniae* thus indicated the broad spectrum antibacterial nature. The two most potent polymers **1c** and **2c** showed MIA values of 0.32 μg/mm^2 and 0.06 μg/mm^2 against MRSA, 0.12 μg/mm^2 and 0.06 μg/mm^2 against VRE and 15.6 μg/mm^2 and 7.8 μg/mm^2 against beta-lactam resistant *K. pneumoniae* respectively (Table 1).

To simulate the natural deposition of airborne bacteria onto surface, a suspension of the human pathogenic bacteria in PBS buffer (pH 7.4) was sprayed onto non-coated (control) and the polymer-coated glass surfaces.[39] The slides were incubated at 37 ˚C for 24 h along with suitable agar to allow the bacterial growth. As expected, non-coated glass surface showed the presence of bacterial colonies thereby indicated the bacterial growth. However, less or no bacterial colony was observed on polymer-coated surfaces depending on the amount painted onto surface. For example, surfaces coated with **2c** (having $-C_{16}H_{33}$ long chain and DQ of 48%) showed (55 ± 5)%, (85 ± 7)%, and 100% reduction of viable *S. aureus* at 0.04 μg/mm^2, 0.08 μg/mm^2 and 0.15 μg/mm^2 with respect to non-coated glass

surface. Similarly **2c** coated surface showed (15 ± 9)%, (45 ± 6)%, (75 ± 5)% and 100% reduction of viable *E. coli* at 0.15 μg/mm^2, 0.3 μg/mm^2, 0.6 μg/mm^2 and 1.2 μg/mm^2 (Figure S11). Notably, polymer **1b** and **1c**-coated surfaces showed complete reduction of viable bacterial (100% activity) at 0.6 μg/mm^2 and 0.3 μg/mm^2 against *S. aureus* and, at 2.6 μg/mm^2 and 1.5 μg/mm^2 against *E. coli* respectively. Polymers **2a**, **2b** and **2c**-coated surfaces, on the other hand, exhibited 100% activity at 1.2 μg/mm^2, 0.6 μg/mm^2 and 0.15 μg/mm^2 against *S. aureus* and at 2.4 μg/mm^2, 2.4 μg/mm^2 and 1.2 μg/mm^2 against *E. coli* respectively. Polymers **3a**, **3b** and **3c** coated surfaces though showed 100% activity at 1.2 μg/mm^2, 0.6 μg/mm^2 and 0.3 μg/mm^2 against *S. aureus* but found to be inactive against *E. coli* till 12 μg/mm^2. Among all the polymers, **1c** and **2c** were found to be the two most active polymers against both the bacteria (Figure 1a and 1b). The high antibacterial activity of these polymers against both Gram-positive and Gram-negative bacteria thus demonstrated that these polymers could be potentially used as bactericidal paint in healthcare settings. Interestingly, polymer **2c** when coated onto the glass surface along with medically relevant polymer such as polylactic acid (PLA) showed antibacterial activity. It is noteworthy that the chitin polymers even after loading with PLA were found to be equally active (e.g., 100% activity was observed for 0.15 μg/mm^2 of **2c** along with 2.5 μg/mm^2 of PLA against *S. aureus* and 1.2 μg/mm^2 of **2c** along with 2.5 μg/mm^2 of PLA against *E. coli* respectively) (Figure 1c and 1d). These findings thus furnished that these chitin polymers could be used to develop self-defensive biomaterials.

2.3. Mechanism of Action. Cationic polymers, e.g., cationic antimicrobial peptides are known to interact with the negatively charged bacterial cell membrane thereby disrupt the membrane-integrity.[40-42] The mode of action of the surface-immobilized cationic chitin polymers were therefore studied against both *S. aureus* and *E. coli*. Sustaining membrane potential is an essential criterion for the bacteria to survive. The dissipation of the membrane

potential was thus studied using a potential sensitive dye $DiSC_3(5)$ (3,3′-dipropylthiadicarbocyanine iodide).[43] All the polymers were found to depolarize the membrane potential of both the bacteria (Figure 2a and 2b). The extent of depolarization was found to depend on degree of quaternization (DQ) and length of alkyl chain. Comparing the membrane depolarization ability of polymers containing the same alkyl chain length ($-C_{16}H_{33}$) but varying DQ (**1c**, **2c** and **3c**), it was observed that the polymer with 48% DQ (**2c)** was the most efficient. In case of polymers with same DQ but varying alkyl chain length (**2a**, **2b** and **2c**), **2c** (with $-C_{16}H_{33}$ alkyl chain) was the most effective in depolarizing the *S. aureus* cell membrane (Figure 2a). On performing a similar study against *E. coli*, with the polymers of constant chain length but variable DQ (**1b**, **2b** and **3b**), **1b** (DQ = 39%) was most efficient. Polymers with same DQ and varying the alkyl chain length (**2a**, **2b** and **2c**), on the other hand, **2a** ($-C_{12}H_{25}$) was most effective in depolarizing the membrane potential of *E. coli* (Figure 2b**)**. However, polymers with higher DQ (**3a-3c**) were found to be less effective in dissipating membrane potential of both the bacteria. The above results were in agreement with the antibacterial efficacy displayed by these polymers. To further substantiate the mode of action of these polymers, leakage of intracellular K^+ ion was studied using potassium ion sensitive dye, PBFI-AM against both *S. aureus* and *E. coli* respectively.[44] All the polymers were found to cause leakage of intracellular K+ ion from both the bacteria and a similar structure activity relationship was observed in case of K^+ ion leakage as observed for membrane depolarization (Figure 2c and 2d). The mode of action of was further examined by fluorescence microscopy via live and dead assay using SYTO 9 and propidium iodide (PI) respectively. SYTO 9, a membrane-permeable green fluorescent dye, is known to bind with the nucleic acid of bacteria and stain with green fluorescence.[45] PI, on the other hand, is a membrane impermeable red fluorescent dye and cannot stain live bacteria. However, it can bind with the nucleic acid of membrane-compromised bacteria and stain with red fluorescent.

The fluorescence microscopy images of non-treated samples showed green fluorescence for both *S. aureus* and *E. coli* thereby indicated the cell viability in control samples (Figure S12a and S12c). However, images of the cells treated with the **2c**-coated surface showed red fluorescence of PI thereby indicated membrane disruption for both *S. aureus* and *E. coli* (Figure S12b and S12d). To visualize the morphological changes in the treated bacteria, scanning electron microscopy (SEM) was used to image both **2c**-treated and non-treated bacteria.[46] The SEM images of the untreated bacteria showed smooth and well-defined surface characteristic of unperturbed bacteria against both *S. aureus* and *E. coli* respectively (Figure S13a and S13c). On the other hand, treated bacteria showed rough and deformed cell surface thereby indicated perturbation of the cell surface for both *S. aureus* and *E. coli* respectively (Figure S13b and S13d).

2.4. Antibiofilm activity. It is estimated that almost 80% of the infections in human occurs due to the biofilm formation.[3,4] Bacterial contamination onto surfaces and subsequent colonization can results in into surface-associated communities known as biofilms. Biofilms are protected by extracellular polymeric substances (EPS) and pose a significant barrier to host immune systems and antibiotics because of the impermeable and defensive EPS.[5] Thus preventing bacterial biofilm formation would indirectly help in inhibiting infections. While the quaternary ammonium moiety containing resin based materials were shown to possess potent antibiofilm activity, we evaluated the antibiofilm properties by coating the polymers onto glass surface and determining efficacy of the polymers in inhibiting bacterial biofilm formation.[47] Glass cover slips coated with the most active polymer **2c** at two different amounts (MIA and 6 × MIA) were challenged against both *S. aureus* and *E. coli* respectively. The cover slips were then imaged by confocal laser scanning microscopy (CLSM). The non-coated cover slips showed huge bacterial growth with an effective thickness of 16-20 μm thus indicating thick and matured biofilm formation for both *S. aureus* and *E. coli* respectively

(Figure 3a and 3d). In contrast, the polymer was also able to inhibit biofilm formation at its MIA values against both *S. aureus* and *E. coli* (Figure 3b and 3e) thereby signifies the potential in inhibiting the biofilm formation. Interestingly, polymer-coated surfaces showed fewer bacteria with an effective thickness of 2-4 μm thereby indicating the presence of only mono-layered bacteria at 6 × MIA values against both *S. aureus* and *E. coli* respectively (Figure 3c and 3f). The above results thus indicated that the cationic chitin polymer prevents bacterial colonization onto the surface.

2.5. Biocompatibility. Hemolysis caused by antibacterial polymer-modified biomaterial surfaces is a major concern for the application in healthcare settings. Hemocompatibility of the polymer coated surfaces was therefore determined with human erythrocytes and was expressed as HA_{50} (the amount of the coated polymer that caused 50% hemolysis).[48] The polymers were found to be non-hemolytic upto 7.8 μg/mm^2. Only 20-30% hemolysis was observed even at 31.2 μg/mm^2 of polymer paint (Figure 4a). Notably, **1c** and **2c**, the two most active polymers caused negligible hemolysis up to 12.5 μg/mm^2 which was much higher compared to their MIA values (Table 1). These results thus indicated the polymers are selectively active toward bacteria. To visualize the effect, both treated and non-treated hRBC were also imaged microscopy (Figure 4b). The images show RBCs taken from polymer coated wells as well as from the tissue culture treated plate (TCTP) control surface. Cells displayed characteristic healthy and round morphology, indicating that the polymer-coated surfaces are non-hemolytic. In contrast, when the highly toxic detergent Triton X (0.5%, v/v) was added, full hemolysis was observed as no hRBC was seen under the microscope. To strengthen the selectivity of these polymers, cytotoxic activity of the most potent polymer **2c** coated surface was performed against human embryo kidney (HEK 293) cells using optical microscopy (Figure S14). Cells were treated with different amounts of **2c** (at lower MIA 0.06 μg/mm^2 and higher MIA 3.9 μg/mm^2 respectively). While the untreated cells showed spindle

shape indicative of healthy morphology (Figure S14a), treated cells at both the amounts were found to retain their morphology (Figure S14b and S14c) and were almost identical with the untreated cells. However, when the cells were treated with highly toxic Triton X, they were found to be of completely spherical shape (Figure S14d). However, cells treated with the higher amount of **2c** seemed to be under stressed condition as the cells were found to be of lees spindle shape. However, these results emphasized that the chitin derivatives are non-toxic at their MIA values.

2.6. *In vitro* and *In vivo* Biodegradation. Common disinfectants that are used to combat infections are becoming more and more useless as the disinfectants cause development of resistance in bacteria and toxic effects towards mammalian cells. Further, non-degradable antimicrobials can create hindrance in tissue-implant integration and unwanted immune responses from host.[31] One potentially effective strategy to reduce infection and to avoid aforementioned problems would thus be, where appropriate, to use degradable materials. To establish the degradability of the cationic chitin derivatives, a thin film of the polymers was prepared onto cover slip and treated with the lysozyme over a period of time. All the tested polymers (**1b**, **1c** and **2c**) were found to degrade in the presence of lysozyme under *in vitro*. The length of the alkyl chain (tetradecyl in **1b** *vs* hexadecyl in **1c**) or the extent of DQ (39% in **1c** *vs* 48% in **2c**) found to have minimal effect on the rate or degree of hydrolysis at the experimental conditions (Figure 5a). The polymers when implanted subcutaneously in rats were also shown to be degradable. Polymer **1b** showed ~20% degradation as compared ~16% and ~15% degradation of **1c** and **2c** after 4 weeks of implantation (Figure 5b). Overall, the rate of degradation of the polymers was much slower probably due to the chemical modifications of chitin.[37] The polymer discs were also imaged by scanning electron microscopy to visualize the morphological changes of the surfaces of discs due to degradation. The treated discs showed porous structures with holes as compared to the non-

treated polymer disc after day 14, 21 and 28 (Figure 5c-f). Further, it was observed that with time both the number of pores and pore size increased thereby indicating the gradual degradation of the polymer under *in vivo* conditions (Figure 5g-j).

2.6. *In vivo* Activity and Biofilm Inhibition. While many polymers display potent *in vitro* antibiofilm efficacy, lack of activity under more complex *in vivo* conditions has been one of the major drawbacks for the antibacterial polymers. Herein *in vivo* antibacterial and antibiofilm efficacies of the polymers were assessed by implanting medical grade polymer-coated catheters (polyurethane, 5 Fr, 12 mm) subcutaneously in mice against methicillin-resistant *S. aureus* (MRSA) infection-one of the most leading biofilm forming bacteria in healthcare and clinical settings.[49] Catheter samples were given bacterial load of ~1.7×10^7 CFU of MRSA at the time of implantation in mice (a quantity greater than that would be encountered in clinical settings). After 96 h, the control samples showed bacterial burden of 7.4 log CFU/catheter thereby showed the prevalence and growth of MRSA. On the other hand, the coated catheter samples showed reduction in bacterial count depending on the amount of the polymer coated. Catheter coated with ~2.5 μg/mm^2 of the polymer showed 1.2 log reduction in bacterial count ($p = 0.0232$) whereas coated-catheter with 5.0 μg/mm^2 of polymer showed a reduction of 2.5 log CFU of MRSA ($p = 0.013$). However, catheter coated with 7.5 μg/mm^2 of polymer showed 3.7 log CFU of MRSA reduction with significant p value ($p < 0.0001$) (Figure 6a). To see bacterial prevalence in the surrounding tissue of the contaminated catheter, tissue samples surrounding catheter were also collected and analysed for cell counting. It was observed that the tissue samples surrounding to 2.5 μg/mm^2 coated catheter displayed only 1.7 log reduction compared to control. However, the tissue samples surrounding to 5.0 μg/mm^2 and 7.5 μg/mm^2 **2c**-coated catheters showed significant bacterial reduction compared to control (2.7 log and 3.5 log of bacterial reduction (p values are 0.0001 and <0.0001) (Figure 6b). Finally, to evaluate the potential of the polymer coating in

inhibiting bacterial biofilm formation, we visualized the implanted catheter using SEM. Uncoated catheter displayed large amount of bacteria in multiple layers thus indicated a thick biofilm formation (Figure 6c). In contrast, polymer coated catheter (at 7.5 μg/mm^2) revealed a fewer amount of bacteria with no cell clusters thus indicating no biofilm formation onto the surface (Figure 6d). The above results thus portrayed the efficacy of the polymer coatings in killing bacteria and inhibiting biofilm inhibition under *in vivo* conditions.

3. CONCLUSIONS

In conclusion, we demonstrated a simple method of developing biodegradable bactericidal paint based on water-insoluble and organo-soluble cationic hydrophobic chitin polymers. The surfaces coated with polymers killed both drug-sensitive and drug-resistant bacteria. The polymers showed excellent compatibility with other polymers suitable for developing self-defensive biomaterials. The hydrophobically modified polymers were shown to inactivate bacteria by disrupting their cell membrane-integrity. Importantly, surfaces coated with the polymers inhibited bacterial biofilm formation on them. Moreover, the polymers were found to be non-hemolytic and showed negligible toxicity against mammalian cells. Catheter coated with the polymer not only reduced MRSA burden but also displayed excellent efficiency in inhibiting bacterial biofilm formation under *in vivo* conditions. Moreover, both *in vitro* and *in vivo* studies showed that the polymers were slowly degradable in the presence of enzymes. Thus the biocompatible and biodegradable coatings developed herein bears potential to be used as antibacterial paint to prevent device-associated infections.

4. EXPERIMENTAL SECTION

4.1. Materials and Instrumentation. Chitin with a degree of acetylation ~75% and potassium hydroxide (KOH) were purchased from SD Fine, India. *N,N*-

dimethyldodecylamine was purchased from Across Organics, Belgium. Lithium chloride (LiCl), potassium bromide (KBr), triethylamine (NEt_3), acetic anhydride (Ac_2O), p-toluene sulfonylchloride (TsCl), *N,N*-dimethyltetradecylamine, *N,N*-dimethylhexadecylamine and anhydrous *N,N* dimethylacetamide (DMAc) were obtained from Sigma-Aldrich, USA. Anhydrous dimethyl sulfoxide (DMSO), anhydrous diethylether (Et_2O) and all other solvents were purchased from Spectrochem, India and were of analytical grade. Methanol was dried with calcium hydride and stored over 4Å molecular sieves. Triethylamine was dried with KOH and stored over KOH. Bacterial strains *S. aureus* (MTCC 737), *E. coli* (MTCC 443) and *P. aeruginosa* (MTCC 424) were purchased from MTCC (Chandigarh, India). Vancomycin-resistant *E. faecium* (VRE) (ATCC 51559), methicilin-resistant *S. aureus* (MRSA) (ATCC 33591) *β*-lactam-resistant *K. pneumoniae* (ATCC 700603) were obtained from ATCC (Rockvillei, Md). Nuclear magnetic resonance spectra (^{1}H NMR) were recorded on a Bruker AMX-400 instrument (400 MHz) in deuterated solvents. Infra red spectra of the polymers were recorded on a Bruker IFS66 V/s spectrometer using potassium bromide pellets. Thermo Finnigan FLASH EA 1112 CHNS analyzer was used to perform elemental analysis of the polymers. Molecular weights of the polymers were recorded by Gel permeation chromatography (GPC) on a Shimadzu-LC 20AD instrument. Polymer coatings and paints were made by a WS5000 spin coater, Techno India, India. Optical density (OD) values were measured by a TECAN (Infinite series, M200) Plate Reader. Eppendorf 5810R centrifuge was used for bacterial centrifugation. Bacterial imaging was performed using a Leica DM2500 fluorescent microscope. A Zeiss 510 Meta confocal laser scanning microscope was used for confocal microscopy imaging.

4.2. Synthesis of Tosyl-chitin. Synthesis of tosylchitins was performed following previously reported protocol with slight modification.[38] Briefly, chitin (2.0 g, equivalent to ~10 mmol of pyranose unit) and lithium chloride (LiCl, 5.2 g) dried at 80 ˚C overnight and at 130 ˚C for 4

h respectively and then were taken in a three-necked round bottom flask fitted with rubber septa. The flask was purged with oxygen-free nitrogen, and anhydrous *N,N*-dimethylacetamide (DMAc) (104 mL) was added. The mixture was then stirred at room temperature until all the solids were dissolved. To the resultant solution was added dry NEt_3 (28.8 mL, 208 mmol) and the flask was transferred to a cold reaction chamber at 8 ˚C. A solution of tosyl chloride (38.12 g, 200 mmol) in DMAc (48 mL) was added to the reaction mixture and the reaction was allowed to proceed for either 24 h or 48 h or 72 h at the same temperature. At the end, the reaction mixture was filtered to remove the insoluble solid and to the filtrate, excess acetone was added to obtain tosylchitin as yellowish white color precipitate. The precipitate was filtered and washed successively with methanol (100 mL × 4), water (100 mL × 4), and acetone (100 mL × 4). Tosylchitin powder (2.5 g) was acetylated by acetic anhydride (1000 μL or 925 μL or 860 μL for tosylchitins obtained after 24 h or 48 h or 72 h of tosylation respectively) in dry methanol (50 mL) overnight. Acetylated tosylchitin (2.0 g) was then treated with methanolic potassium hydroxide (45 mL or 50 mL or 55 mL, 0.1 N KOH for tosylchitins obtained after 24 h or 48 h or 72 h of tosylation respectively) for 3 h at room temperature to give *N*-acetylated tosyl-chitin. The *N*-acetylated tosyl-chitins were characterized by ^{1}H NMR and elemental analysis. The degree of tosylation (DS) was calculated as the ratio of sulfur by nitrogen obtained in elemental analysis (DS = S/N × 100%) (1). The tosylchitins obtained after acetylation and subsequent base treatment is referred as tosylchitin (Tsch). The tosylchitins obtained after 24 h, 48 h and 72 h were referred as Tsch 1, Tsch 2 and Tsch 3 respectively.

4.3. Synthesis of Quaternized Chitin Polymers. Tosylchitins (1.0 g) with different degrees of tosylation were first dissolved in anhydrous *N,N*-dimethyl acetamide (DMAc) (30 mL) in sealed screw-top pressure tube. To the reaction mixture was added *N,N*-dimethylalkylamines (10 equivalent per tosylated sugar unit) and the reaction was allowed to proceed at 120 ˚C

for 72 h. After the reaction, diethyl ether was added in excess (150 mL) to precipitate the quaternized chitin derivatives. The precipitate was filtered through a sintered glass funnel and was washed repeatedly with diethyl ether to obtain pure quaternary chitin derivatives with 100% degree of quaternization (with respect to tosyl groups for each tosylchitin). Finally the precipitates were dried in vacuum oven to give colorless/faint yellowish products with 70-80% yield. The quaternary chitin derivatives were characterized by FT-IR, ^{1}H NMR and elemental analysis.

4.4. Gel Permeation Chromatography. The products were further characterized by gel permeation chromatography (GPC). Molecular weights and polydispersities were determined on a Shimadzu-LC 20AD instrument with refractive index detector using a phenogel 5μ 10E5A column (300 × 7.8 mm-Part No. 00H-0446-K0). GPC samples were run in *N,N*-dimethylacetamide solvent as mobile phase (flow rate of 1 mL/min). Seven different molecular weight pullulan standards obtained from Sigma-Aldrich (USA-catalogue 96351) were used for calibration in GPC. The range of pullulan standards was from 10 to 805 kDa (10, 21.7, 48, 113, 200, 366 and 805 kDa). The molecular weights reported are relative to these standards.

4.5. Solubility of the Chitin Derivatives. Solubility of the quaternary chitin derivatives were checked in both aqueous and various organic solvents. The details of the method were given in the Supporting Information.

4.6. Preparation of the Paint. Chitin derivatives were first dissolved in methanol (50 mg/mL) and the solutions were serially diluted (2-fold serial dilution) in methanol. The organic solutions (20 μL) of serial dilutions were added into the flat-bottom wells of 96-well plate. The plate was first kept for air-drying and then dried in vacuum oven overnight at 60 ˚C to get film onto the surface of the wells of well plate. For determining the antibacterial activity against water-borne bacteria, each well was coated in triplicate for all the

concentrations of all the polymers. For determining the antibacterial activity against air-borne bacteria, films on microscopic glass slides were prepared by spin coating using solutions of chitin derivatives in methanol and chloroform mixture (MeOH: $CHCl_3$ = 1:9, 350 μL). Films of these derivatives were also prepared along with the polymers such polylactic acid (PLA) from the mixed solution (350 μL) of PLA in chloroform and chitin derivatives in MeOH ($CHCl_3$: MeOH = 9:1) using spin coater. For the biodegradation study, thin films of the chitin derivatives were prepared on microscopic cover glass (18 mm). To prepare the film, required amount of chitin derivative (**2c**) was dissolved in DMSO and 160 μL of the solution was drop casted on cover glass and dried in oven at 70 ˚C overnight. The amount of the polymers coated onto surfaces was expressed as $\mu g/mm^2$.

4.7. Antibacterial Activity against Water-borne Bacteria. Antibacterial activity of the polymers was determined by adding bacterial suspension in suitable broth (200 μL of ~10^5 CFU/mL) to the polymer-coated wells of 96-well plates. Two negative controls were made while coating the polymers: solvent free wells (blank wells) as one set of control and the other where 20 μL of the only solvent coated wells (to see the effect of solvent on bacterial growth). The plates with the bacterial suspension were then incubated at 37 ˚C in a shaker incubator for 24 h. The wells which did not show any visual turbidity was noted and the amount present in the wells were used to calculate the minimum inhibitory amount for the respective bacteria. The minimum amount required per unit surface area to inhibit the growth of the bacteria was then reported as the minimum inhibitory amount (MIA) ($\mu g/mm^2$) (considering the area of the wells of tissue culture plates).

4.8. Antibacterial Activity against Air-borne Bacteria. Bacteria were grown in suitable media for 6 h (~10^9 CFU/mL). Then 1 mL of the culture was centrifuged (at 12000 rpm for about 1 min) to harvest bacteria which were then washed with 1 mL of phosphate buffered saline (PBS, pH 7.4). Finally, bacteria were resuspended in PBS and diluted to ~10^7 CFU/mL

and ~10^6 CFU/mL for *S. aureus* and *E. coli* respectively. Bacterial suspension was then sprayed onto the coated or non-coated glass slides (2.5 cm × 5.5 cm) by a chromatography sprayer (spray rate ~10 mL/min) (3). The slides with the bacterial droplets were then allowed to get dried in air for about 2-3 min and cautiously transferred into petridishes. Suitable agar slabs were then gently placed onto the slides and the pertidishes were sealed and kept at 37 ˚C for about 24 h till visible bacterial colonies observed. Cell biosciences gel documentation instrument were used to image the glass slides with or without bacterial colonies using white light. Alpha-imager software was used to process images. A non-coated glass slide was used similarly as a negative control.

4.9. Mechanism of action. The mode of action of the cationic chitin derivatives were studied by membrane depolarization assay, intracellular potassium ion leakage assay, live and dead assay via fluorescence microscopy and visual inspection by scanning electron microscopy. The details of the method were given in the Supporting Information.

4.10. Biocompatibility. The biocompatibility of the polymeric coatings was evaluated by studying their hemolytic and cytotoxic activity against human red blood cells (hRBC) and human embryo kidney cells (HEK 293) respectively. The details of toxicity studies were provided in the Supporting Information.

4.11. Biofilm Inhibition Assay. First, the glass cover slips (18 mm) were coated with different amount of **2c** and were placed into the wells of a 6-well plate. *S. aureus* and *E. coli* (6 h grown, ~10^9 CFU/mL) were diluted to ~10^5 CFU/mL into suitable broth (nutrient broth supplemented with 1% NaCl and glucose and M9 broth supplemented with 0.5% glycerol and 0.02% casamino acid for *S. aureus* and *E. coli* respectively). Bacterial suspensions (2 mL) were added to the wells containing the polymer coated cover slips and incubated at 37 ˚C under stationary condition. A similar experiment was performed by placing 2 mL of respective bacterial suspensions to the wells containing an uncoated cover slip as negative

control. Cover slips were then removed and washed carefully once with PBS. Finally cover slips were taken on a glass slide and green fluorescent dye SYTO 9 (15 μL, 3 μM) was added to the cover slip. The experimental cover slip was then covered by another cover slip, air-sealed and incubated in dark for 15 min. Both non-treated and treated cover slips were then imaged using a Zeiss 510 Meta confocal laser scanning microscope. The excitation and emission wavelengths for SYTO 9 were 488 nm and 500-550 nm respectively.

4.12. *In vitro* Biodegradation. Microscopic cover slip (18 mm) were coated with the known amount of polymers **1b**, **1c** and **2c** following the coating procedure as described previously. The cover slips were placed in a 6-well plate (the weight of uncoated and the polymer-coated cover slips were recorded to calculate the coating amount). Phosphate buffer saline (PBS, pH = 7.2) was used for this study and the enzyme was chicken egg lysozyme (≥ 40,000 units/mg protein). Lysozyme was dissolved in the PBS to give an enzyme concentration of 4 mg/mL and then was added (4 mL) to the wells of 6-well plate containing coated cover slips. As control experiment, another polymer coated cover slip was placed in enzyme-free buffer-solution. The samples were incubated in a shaker incubator at 37 ˚C for 28 days under constant agitation. The cover slips were then removed at different time intervals from the plates, washed with Millipore water and dried in a vacuum oven till its weight remained unchanged. The weights of the dried cover slips were recorded and the extent of hydrolysis was calculated as % of the weight loss of the film after lysozyme treatment.

4.13. *In vivo* Degradation. *In vivo* degradation was performed with wistar rats following the protocols approved by the Institutional Animal Ethics Committee (IAEC) in Jawaharlal Nehru Centre for Advanced Scientific Research. In each group, a total of five male wistar rats weighing 250-350 g were used. The rats were anesthetized with ketamine (100 mg/kg) and xylazine (5 mg/kg) intra-peritoneally. The backs of the rats were shaved aseptically. A midline incision was then made in the skin above the mid-thoracic spine and a subcutaneous

(s.c.) pouch was created by blunt dissection extending in each rat interiorly. Polymer discs (11 mm of diameter) of the polymers (**1b**, **1c** and **2c**) of known weight (40-60 mg) were made by a hydraulic press. Next the discs were sterilized by UV irradiation, soaked in sterile PBS for about 1 h (pH 7.4) prior to implantation and inserted into the s.c. pouch of rat. The incision was then closed with silk suture (6.0). After definite time intervals, the rats were killed and the polymer disc samples were harvested. The samples were then rinsed with Millipore water and dried to a constant weight at 60 ˚C in a vacuum oven. Finally the weight of the dried disc samples was recorded. The extent of *in vivo* degradation was expressed as the percentage of the weight loss of after implantation. Further, to visualize the surface morphology of the disc, discs were gold coated and imaged by Quanta 3D FEG FEI scanning electron microscope.

4.14. *In vivo* Activity. *In vivo* activity of the polymer was evaluated by coating medical grade catheters and subsequently contaminating the coated catheters. Polyurethane catheters (5-French) were used and cut into pieces (12 mm length, average weight ~25 mg). The catheter pieces were then heat sealed on both ends and was dip-coated with different amounts of the most active polymer **2c** (~2.5 μg/mm^2, 5.0 μg/mm^2, and 7.5 μg/mm^2). BALB/c mice weighing 18-22 g (6-8 weeks old) were used according to protocols approved by the Institutional Animal Ethics Committee (IAEC) in the institute (Jawaharlal Nehru Centre for Advanced Scientific Research). In each group, a total of five mice were used. Mice were anesthetized with ketamine (40 mg/kg) and xylazine (2 mg/kg of xylazine). The hair at the back of each mouse was clipped and then shaved aseptically. A midline incision was then made in the skin above the mid-thoracic spine and a subcutaneous (s.c.) pouch was created by blunt dissection extending interiorly in each mouse. Polymer coated catheters were inoculated with ~6.9 × 10^7 CFU/mL MRSA and incubated under stationary conditions at 37 ˚C for 90 min to allow the adherence of the bacteria. The bacteria contaminated catheters were then

placed in the s.c. pockets of mice. The incisions were closed with 3.0 vicryl sutures and the mice were allowed to have access of food and water. After 96 h, mice were killed by isoflurane and the coated catheters were removed aseptically and placed in eppendrof tubes containing 1 mL of nutrient broth. Then the broth containing catheter samples was sonicated for 3 min in a water bath sonicator (550 W, 37,000 Hz; S 60H Elmasonic sonicator) followed by another 2 min sonication under same condition. The nutrient broth was serially diluted in saline and plated on agar plate to determine the number of viable bacteria. A similar experiment was performed by taking non-coated catheter as control. The number of viable bacteria present in the experimental catheter samples was represented as logCFU/catheter. Bacterial count was also determined in the surrounding tissues after collecting, homogenizing and plating the tissue sample on suitable agar plates. For SEM imaging, the catheter samples after removing from mice was placed in formalin for 24 h and then dehydrated with subsequent treatment of 30, 50, 70, 90 and 100% of ethanol. Finally the catheter pieces were imaged by FESEM after sputter coated with gold.

Supporting Information. Details of characterization, FT-IR and ^{1}H NMR spectra of the polymers, solubility of the polymers, procedures of mechanistic studies, tables and figures showing physical and antibacterial properties of the polymers. The Supporting Information is available free of charge on the ACS Publications website.

AUTHOR INFORMATION

Corresponding author: jayanta@jncasr.ac.in

Notes

The authors declare no competing financial interest.

Acknowledgements

We thank Prof. C. N. R. Rao, FRS (JNCASR) for his constant support and encouragement. We also thank Dr. R. G. Prakash for helping in performing vivo experiments. J. Hoque thanks JNCASR for senior research fellowship (SRF). This work was supported by the DST-Fast Track project (SR/FT/CS-097/2009), Department of Science and Technology, Government of India. J. Haldar also acknowledges Ramanujan fellowship (SR/S2/RJN-43/2009) from the Department of Science and Technology, Government of India.

References

1. Darouiche, R. O. Treatment of Infections Associated with Surgical Implants. *N. Engl. J. Med.* **2004,** *350*, 1422-1429.

2. Busscher, H. J.; van der Mei, H. C.; Subbiahdoss, G.; Jutte, P. C.; van den Dungen, J. J.; Zaat, S. A.; Schultz, M. J.; Grainger, D. W. Biomaterial-associated Infection: Locating the Finish Line in the Race for the Surface. *Sci. Transl. Med.* **2012,** *4*, 153rv10.

3. Arciola, C. R.; Campoccia, D.; Speziale, P.; Montanaro, L.; Costerton, J. W., Biofilm formation in Staphylococcus implant infections. A Review of Molecular Mechanisms and Implications for Biofilm-resistant Materials. *Biomaterials* **2012,** *33*, 5967-5982.

4. Salwiczek, M.; Qu, Y.; Gardiner, J.; Strugnell, R. A.; Lithgow, T.; McLean, K. M.; Thissen, H. Emerging Rules for Effective Antimicrobial Coatings. *Trends Biotechnol.* **2014,** *32*, 82-90.

5. Davies, D. Understanding Biofilm Resistance to Antibacterial Agents. *Nat. Rev. Drug Discov.* **2003,** *2*, 114-122.

6. von Eiff, C.; Jansen, B.; Kohnen, W.; Becker, K. Infections Associated with Medical Devices: Pathogenesis, Management and Prophylaxis. *Drugs* **2005,** *65*, 179-214.

7. Hetrick, E. M.; Schoenfisch, M. H. Reducing Implant-related Infections: Active Release Strategies. *Chem. Soc. Rev.* **2006**, *35*, 780-789.

8. Yang, W. J.; Cai, T.; Neoh, K.-G.; Kang, E.-T.; Teo, S. L.-M.; Rittschof, D. Barnacle Cement as Surface Anchor for "Clicking" of Antifouling and Antimicrobial Polymer Brushes on Stainless Steel. *Biomacromolecules* **2013**, *14*, 2041-2051.

9. Song, J.; Chen, Q.; Zhang, Y.; Diba, M.; Kolwijck, E.; Shao, J.; Jansen, J. A.; Yang, F.; Boccaccini, A. R.; Leeuwenburgh, S. C. G. Electrophoretic Deposition of Chitosan Coatings Modified with Gelatin Nanospheres To Tune the Release of Antibiotics. *ACS Appl. Mater. Interfaces* **2016**, *8*, 13785-13792.

10. Wong, S. Y.; Moskowitz, J. S.; Veselinovic, J.; Rosario, R. A.; Timachova, K.; Blaisse, M. R.; Fuller, R. C.; Klibanov, A. M.; Hammond, P. T. Dual Functional Polyelectrolyte Multilayer Coatings for Implants: Permanent Microbicidal Base with Controlled Release of Therapeutic Agents. *J. Am. Chem. Soc.* **2010,** *132*, 17840-17848.

11. Hwang, G. B.; Allan, E.; Parkin, I. P. White Light-Activated Antimicrobial Paint using Crystal Violet. *ACS Appl. Mater. Interfaces* **2016,** *8*, 15033-15039.

12. Han, H.; Wu, J. F.; Avery, C. W.; Mizutani, M.; Jiang, X. M.; Kamigaito, M.; Chen, Z.; Xi, C. W.; Kuroda, K. Immobilization of Amphiphilic Polycations by Catechol Functionality for Antimicrobial Coatings. *Langmuir* **2011,** *27*, 4010-4019.

13. Ivanova, K.; Fernandes, M. M.; Francesko, A.; Mendoza, E.; Guezguez, J.; Burnet, M. Tzanov. T. Quorum-Quenching and Matrix-Degrading Enzymes in Multilayer Coatings Synergistically Prevent Bacterial Biofilm Formation on Urinary Catheters. ACS Appl. Mater. Interfaces **2015**, *7*, 27066-27077.

14. Sileika, T. S.; Barrett, D. G.; Zhang, R.; Lau, K. H.; Messersmith, P. B. Colorless Multifunctional Coatings Inspired by Polyphenols Found in Tea, Chocolate, and Wine. *Angew. Chem. Int. Ed.* **2013,** *52*, 10766-10770.

15. Kumar, A.; Vemula, P. K.; Ajayan, P. M.; John, G. Silver-Nanoparticle-Embedded Antimicrobial Paints Based on Vegetable Oil. *Nat. Mater.* **2008,** *7*, 236-241.

16. Pritchard, E. M.; Valentin, T.; Panilaitis, B.; Omenetto, F.; Kaplan, D. L. Antibiotic-Releasing Silk Biomaterials for Infection Prevention and Treatment. *Adv. Funct. Mater.* **2013,** *23*, 854-861.

17. Demir, B.; Cerkez, I.; Worley, S. D.; Broughton, R. M.; Huang, T. S. N-Halamine-Modified Antimicrobial Polypropylene Nonwoven Fabrics for Use against Airborne Bacteria. *ACS Appl. Mater. Interfaces* **2015,** *7*, 1752-1757.

18. Wang, J.; Li, J.; Qian, S.; Guo, G.; Wang, Q.; Tang, J.; Shen, H.; Liu, X.; Zhang, X.; Chu, P. K. Antibacterial Surface Design of Titanium-Based Biomaterials for Enhanced Bacteria-Killing and Cell-Assisting Functions Against Periprosthetic Joint Infection. *ACS Appl. Mater. Interfaces* **2016,** *8*, 11162-11178.

19. Yang, C.; Ding, X.; Ono, R. J.; Lee, H.; Hsu, L. Y.; Tong, Y. W.; Hedrick, J.; Yang, Y. Y. Brush-like Polycarbonates Containing Dopamine, Cations, and PEG Providing a Broad-Spectrum, Antibacterial, and Antifouling Surface via One-step Coating. *Adv. Mater.* **2014,** *26*, 7346-7351.

20. Milovic, N. M.; Wang, J.; Lewis, K.; Klibanov, A. M. Immobilized N-Alkylated Polyethylenimine Avidly Kills Bacteria by Rupturing Cell Membranes With No Resistance Developed. *Biotechnol. Bioeng.* **2005,** *90*, 715-722.

21. Tiller, J. C.; Liao, C. J.; Lewis, K.; Klibanov, A. M. Designing Surfaces that Kill Bacteria on Contact. *Proc Natl Acad Sci U S A* **2001,** *98*, 5981-5985.

22. Li, P.; Poon, Y. F.; Li, W.; Zhu, H. Y.; Yeap, S. H.; Cao, Y.; Qi, X.; Zhou, C.; Lamrani, M.; Beuerman, R. W.; Kang, E. T.; Mu, Y.; Li, C. M.; Chang, M. W.; Leong, S. S.; Chan-Park, M. B. A Polycationic Antimicrobial and Biocompatible Hydrogel with Microbe Membrane Suctioning Ability. *Nat. Mater.* **2011,** *10*, 149-156.

23. Ista, L. K.; Dascier, D.; Ji, E.; Parthasarathy, A.; Corbitt, T. S.; Schanze, K. S.; Whitten, D. G. Conjugated-Polyelectrolyte-Grafted Cotton Fibers Act as "Micro Flypaper" for the Removal and Destruction of Bacteria. *ACS Appl. Mater. Interfaces* **2011,** *3*, 2932-2937.

24. Cao, Z. Q.; Mi, L.; Mendiola, J.; Ella-Menye, J. R.; Zhang, L.; Xue, H.; Jiang, S. Y. Reversibly Switching the Function of a Surface between Attacking and Defending against Bacteria. *Angew. Chem. Int. Ed.* **2012,** *51*, 2602-2605.

25. Park, D.; Wang, J.; Klibanov, A. M., One-step, Painting-like Coating Procedures to Make Surfaces Highly and Permanently Bactericidal. *Biotechnol. Prog.* **2006,** *22*, 584-589.

26. Haldar, J.; An, D.; Alvarez de Cienfuegos, L.; Chen, J.; Klibanov, A. M. Polymeric Coatings that Inactivate both Influenza Virus and Pathogenic Bacteria. *Proc. Natl. Acad. Sci. USA* **2006,** *103*, 17667-17671.

27. Ravikumar, T.; Murata, H.; Koepsel, R. R.; Russell, A. J., Surface-Active Antifungal Polyquaternary Amine. *Biomacromolecules* **2006,** *7*, 2762-2769.

28. Hoque, J.; Akkapeddi, P.; Yadav, V.; Manjunath, G. B.; Uppu, D. S.; Konai, M. M.; Yarlagadda, V.; Sanyal, K.; Haldar, J. Broad Spectrum Antibacterial and Antifungal Polymeric Paint Materials: Synthesis, Structure-Activity Relationship, and Membrane-Active Mode of Action. *ACS Appl. Mater. Interfaces* **2015,** *7*, 1804-1815.

29. Bieser, A. M.; Tiller, J. C. Mechanistic Considerations on Contact-Active Antimicrobial Surfaces With Controlled Functional Group Densities. *Macromol. Biosci.* **2011,** *11*, 526-534.

30. Sambhy, V.; MacBride, M. M.; Peterson, B. R.; Sen, A. Silver Bromide Nanoparticle/Polymer Composites: Dual Action Tunable Antimicrobial Materials. *J. Am. Chem. Soc.* **2006,** *128*, 9798-9808.

31. Daghighi, S.; Sjollema, J.; van der Mei, H. C.; Busscher, H. J.; Rochford, E. T. J. Infection Resistance of Degradable versus non-Degradable Biomaterials: An Assessment of the Potential Mechanisms. *Biomaterials* **2013,** *34*, 8013-8017.

32. Cado, G.; Aslam, R.; Seon, L.; Garnier, T.; Fabre, R.; Parat, A.; Chassepot, A.; Voegel, J. C.; Senger, B.; Schneider, F.; Frere, Y.; Jierry, L.; Schaaf, P.; Kerdjoudj, H.; Metz-Boutigue, M. H.; Boulmedais, F. Self-Defensive Biomaterial Coating Against Bacteria and Yeasts: Polysaccharide Multilayer Film with Embedded Antimicrobial Peptide. *Adv. Funct. Mater.* **2013,** *23*, 4801-4809.

33. Hsu, B. B.; Park, M. H.; Hagerman, S. R.; Hammond, P. T. Multimonth Controlled Small Molecule Release from Biodegradable Thin Films. *Proc. Natl. Acad. Sci. USA* **2014,** *111*, 12175-12180.

34. Behlau, I.; Mukherjee, K.; Todani, A.; Tisdale, A. S.; Cade, F.; Wang, L.; Leonard, E. M.; Zakka, F. R.; Gilmore, M. S.; Jakobiec, F. A.; Dohlman, C. H.; Klibanov, A. M. Biocompatibility and Biofilm Inhibition of N,N-Hexyl,methyl-polyethylenimine Bonded to Boston Keratoprosthesis Materials. *Biomaterials* **2011,** *32*, 8783-8796.

35. Pavlukhina, S. V.; Kaplan, J. B.; Xu, L.; Chang, W.; Yu, X.; Madhyastha, S.; Yakandawala, N.; Mentbayeva, A.; Khan, B.; Sukhishvili, S. A. Noneluting Enzymatic Antibiofilm Coatings. *ACS Appl. Mater. Interfaces* **2012,** *4*, 4708-4716.

36. Kumar, M. N. V. R.; Muzzarelli, R. A. A.; Muzzarelli, C.; Sashiwa, H.; Domb, A. J. Chitosan Chemistry and Pharmaceutical Perspectives. *Chem. Rev.* **2004,** *104*, 6017-6084.

37. Tomihata, K.; Ikada, Y. In Vitro and In Vivo Degradation of Films of Chitin and Its Deacetylated Derivatives. *Biomaterials* **1997,** *18*, 567-575.

38. Zou, Y. Q.; Khor, E. Preparation of C-6 Substituted Chitin Derivatives Under Homogeneous Conditions. *Biomacromolecules* **2005,** *6*, 80-87.

39. Haldar, J.; Weight, A. K.; Klibanov, A. M. Preparation, Application and Testing of Permanent Antibacterial and Antiviral Coatings. *Nat. Protoc.* **2007,** *2*, 2412-2417.

40. Wang, Y.; Corbitt, T. S.; Jett, S. D.; Tang, Y.; Schanze, K. S.; Chi, E. Y.; Whitten, D. G. Direct Visualization of Bactericidal Action of Cationic Conjugated Polyelectrolytes and Oligomers. *Langmuir* **2012,** *28*, 65-70.

41. Liu, R. H.; Chen, X. Y.; Chakraborty, S.; Lemke, J. J.; Hayouka, Z.; Chow, C.; Welch, R. A.; Weisblum, B.; Masters, K. S.; Gellman, S. H. Tuning the Biological Activity Profile of Antibacterial Polymers via Subunit Substitution Pattern. *J. Am. Chem. Soc.* **2014,** *136*, 4410-4418.

42. Mensa, B.; Kim, Y. H.; Choi, S.; Scott, R.; Caputo, G. A.; DeGrado, W. F. Antibacterial Mechanism of Action of Arylamide Foldamers. *Antimicrob. Agents Chemother.* **2011,** *55*, 5043-5053.

43. Hoque, J.; Konai, M. M.; Gonuguntla, S.; Manjunath, G. B.; Samaddar, S.; Yarlagadda, V.; Haldar, J. Membrane Active Small Molecules Show Selective Broad Spectrum Antibacterial Activity with No Detectable Resistance and Eradicate Biofilms. *J. Med. Chem.* **2015,** *58*, 5486-5500.

44. Yarlagadda, V.; Samaddar, S.; Paramanandham, K.; Shome, B. R.; Haldar, J. Membrane Disruption and Enhanced Inhibition of Cell-Wall Biosynthesis: A Synergistic Approach to Tackle Vancomycin-Resistant Bacteria. *Angew. Chem. Int. Ed.* **2015,** *54*, 13644-13649.

45. Hoque, J.; Konai, M. M.; Samaddar, S.; Gonuguntala, S.; Manjunath, G. B.; Ghosh, C.; Haldar, J. Selective and Broad Spectrum Amphiphilic Small Molecules to Combat Bacterial Resistance and Eradicate Biofilms. *Chem. Commun.* **2015,** *51*, 13670-13673.

46. Hoque, J.; Akkapeddi, P.; Yarlagadda, V.; Uppu, D. S.; Kumar, P.; Haldar, J. Cleavable Cationic Antibacterial Amphiphiles: Synthesis, Mechanism of Action, and Cytotoxicities. *Langmuir* **2012,** *28*, 12225-12234.

47. Ganewatta, M. S.; Miller, K. P.; Singleton, S. P.; Mehrpouya-Bahrami, P.; Chen, Y. P.; Yan, Y.; Nagarkatti, M.; Nagarkatti, P.; Decho, A. W.; Tang, C. B. Antibacterial and

Biofilm-Disrupting Coatings from Resin Acid-Derived Materials. *Biomacromolecules* **2015,** *16*, 3336-3344.

48. Uppu, D. S. S. M.; Samaddar, S.; Ghosh, C.; Paramanandham, K.; Shome, B. R.; Haldar, J. Amide Side Chain Amphiphilic Polymers Disrupt Surface Established Bacterial Biofilms and Protect Mice from Chronic *Acinetobacter baumannii* Infection. *Biomaterials* **2016,** *74*, 131-143.

49. Chen, R.; Willcox, M. D. P.; Ho, K. K. K.; Smyth, D.; Kumar, N. Antimicrobial Peptide Melimine Coating for Titanium and Its In Vivo Antibacterial Activity in Rodent Subcutaneous Infection Models. *Biomaterials* **2016**, *85*, 142-151.

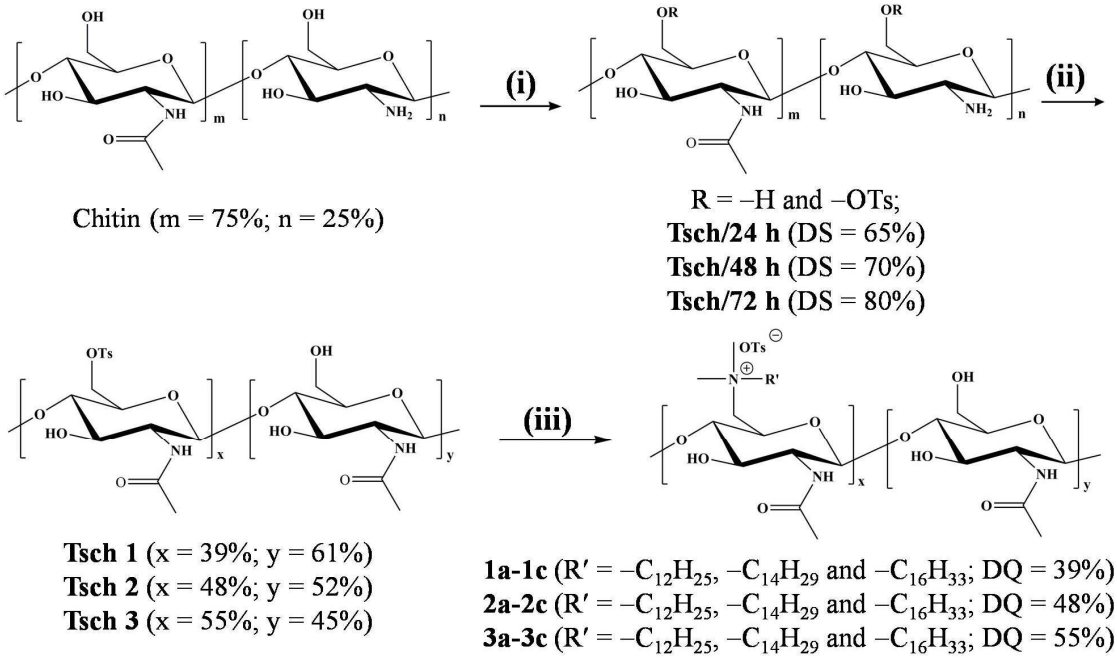

Scheme 1. Synthesis of quaternary hydrophobic chitin polymers: (i) TsCl, NMe_3, DMAc, LiCl, 8 ˚C, 24 h or 48 h or 72 h; (ii) a) Ac_2O, MeOH, RT, 12 h; b) KOH, MeOH, RT, 3 h; (iii) R′NMe_2, dry DMSO/DMAc, 120 ˚C, 72 h. Tsch/24 h, Tsch/48 h and Tsch/72 h are the tosylchitins obtained after tosylation of chitin; Tsch 1, Tsch 2 and Tsch 3 are the tosylchitins obtained after *N*-acetylation and subsequent KOH treatment; DS = Degree of substitution; DQ = Degree of quaternization.

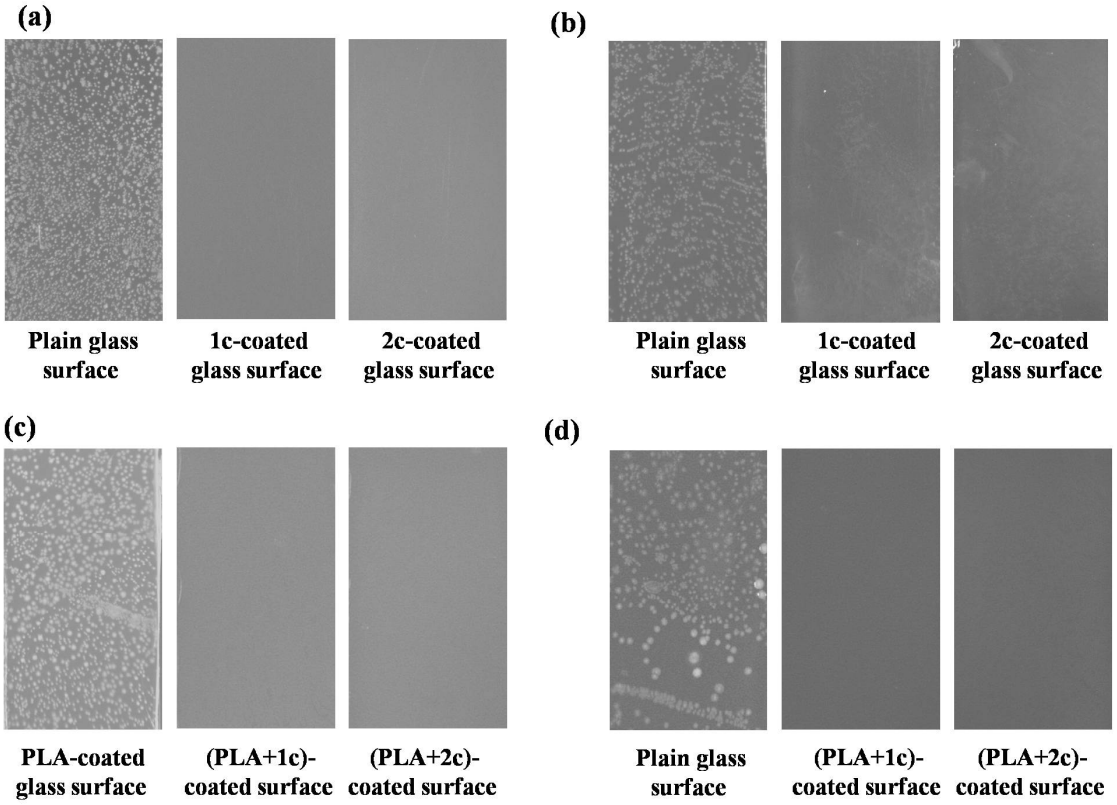

Figure 1. Antibacterial activity of polymer coated surfaces. Photographs of microscopic glass slides after spraying bacteria and incubating for 24 h; left panel of (a) and (b): non-coated glass slides (controls); middle panel of (a) and (b): slides coated with **1c** (0.3 and 1.5 μg/mm^2); right panel of (a) and (b): slides coated with **2c** (0.15 and 1.2 μg/mm^2); left panel of (c) and (d): slides coated with PLA (2.5 μg/mm^2); middle panel of (c) and (d): slides coated with (0.3 μg/mm^2 **1c** + 2.5 μg/mm^2 PLA) and (1.5 μg/mm^2 **1c** + 2.5 μg/mm^2 PLA); right panel of (c) and (d): slides coated with (0.15 μg/mm^2 **2c** + 2.5 μg/mm^2 PLA) and (1.2 μg/mm^2 **2c** + 2.5 μg/mm^2 PLA).

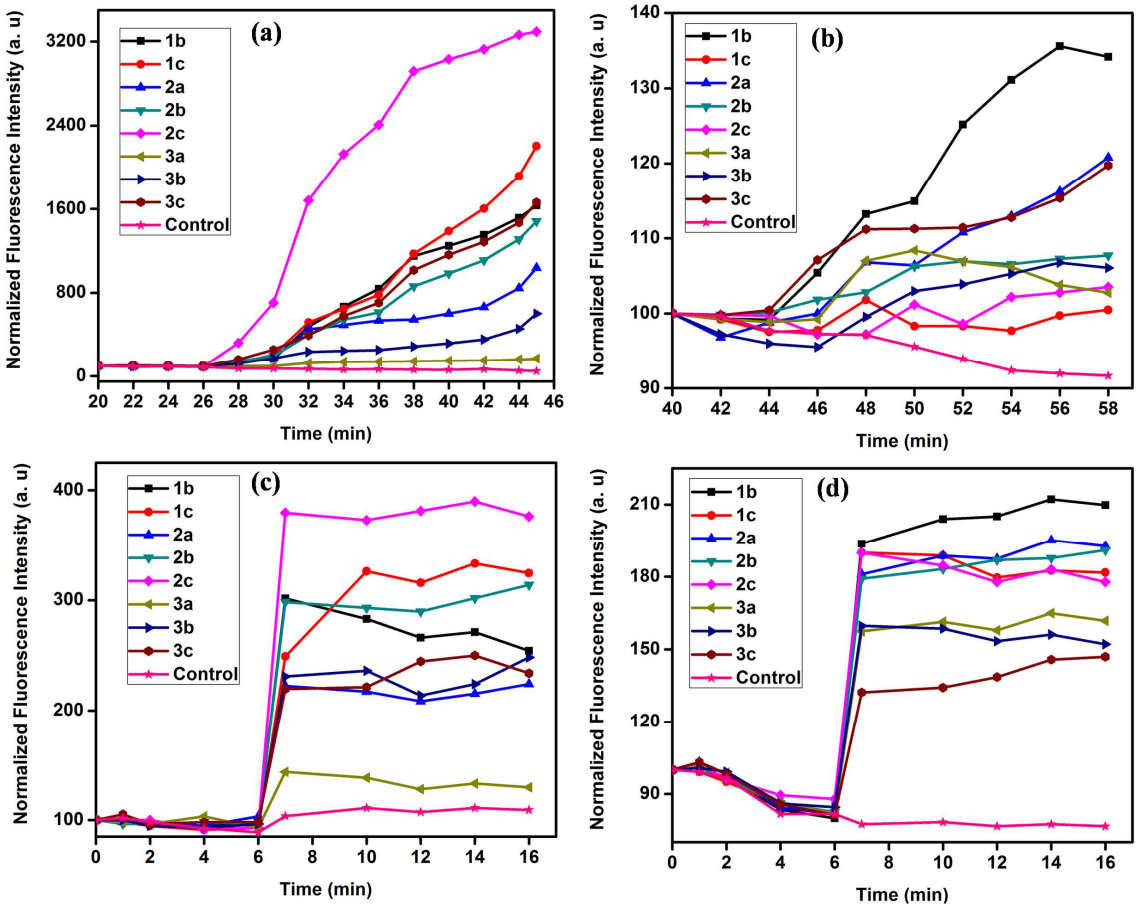

Figure 2. Mechanism of antibacterial action. (a and b) Cytoplasmic membrane depolarization ability of polymers against *S. aureus* and *E. coli*; (c and d) intracellular K^+ ion leakage ability of polymers against *S. aureus* and *E. coli* respectively.

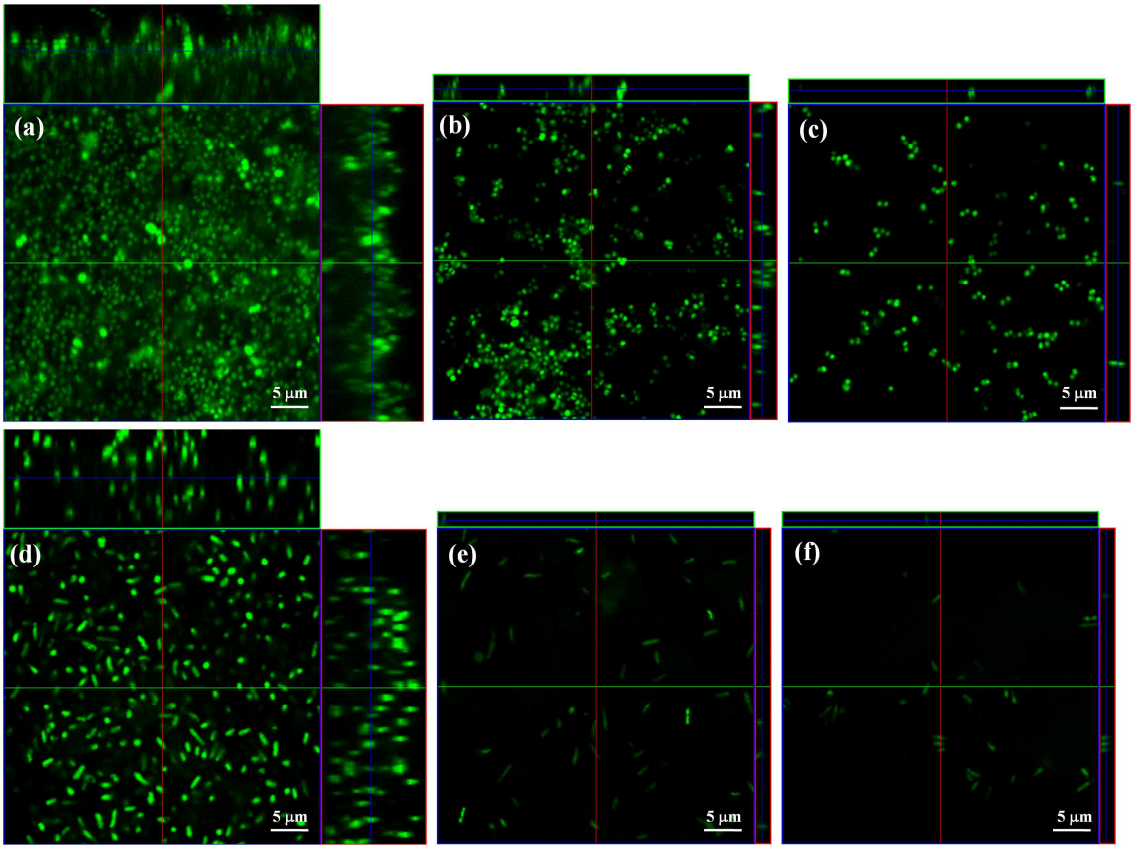

Figure 3. Antibiofilm activity of the polymeric coating. Confocal laser scanning microscopy images of (a and d) non-coated cover glass; (b and e) cover glass coated with 0.06 µg/mm^2 and 3.9 µg/mm^2 and (c and f) with 0.36 µg/mm^2 and 23.4 µg/mm^2 respectively. Upper panel shows for *S. aureus* and lower panel shows for *E. coli* respectively.

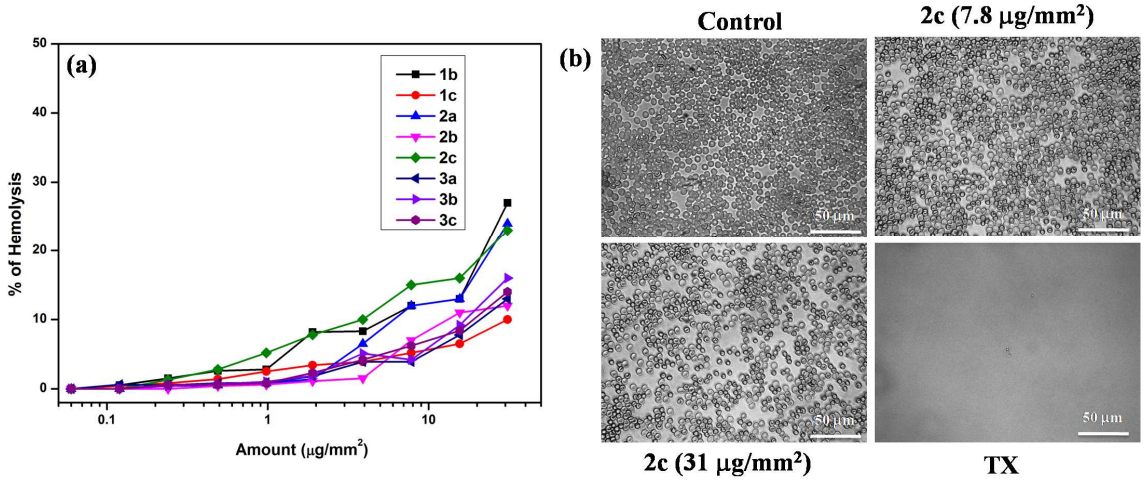

Figure 4. *In vitro* biocompatibility of the polymers. (a) % of Hemolysis of polymers as a function of the amount of polymer-coating; (b) phase-contrast images of erythrocytes taken from the polymer-coated surfaces or from the control TCTP surface with and without Triton X (TX).

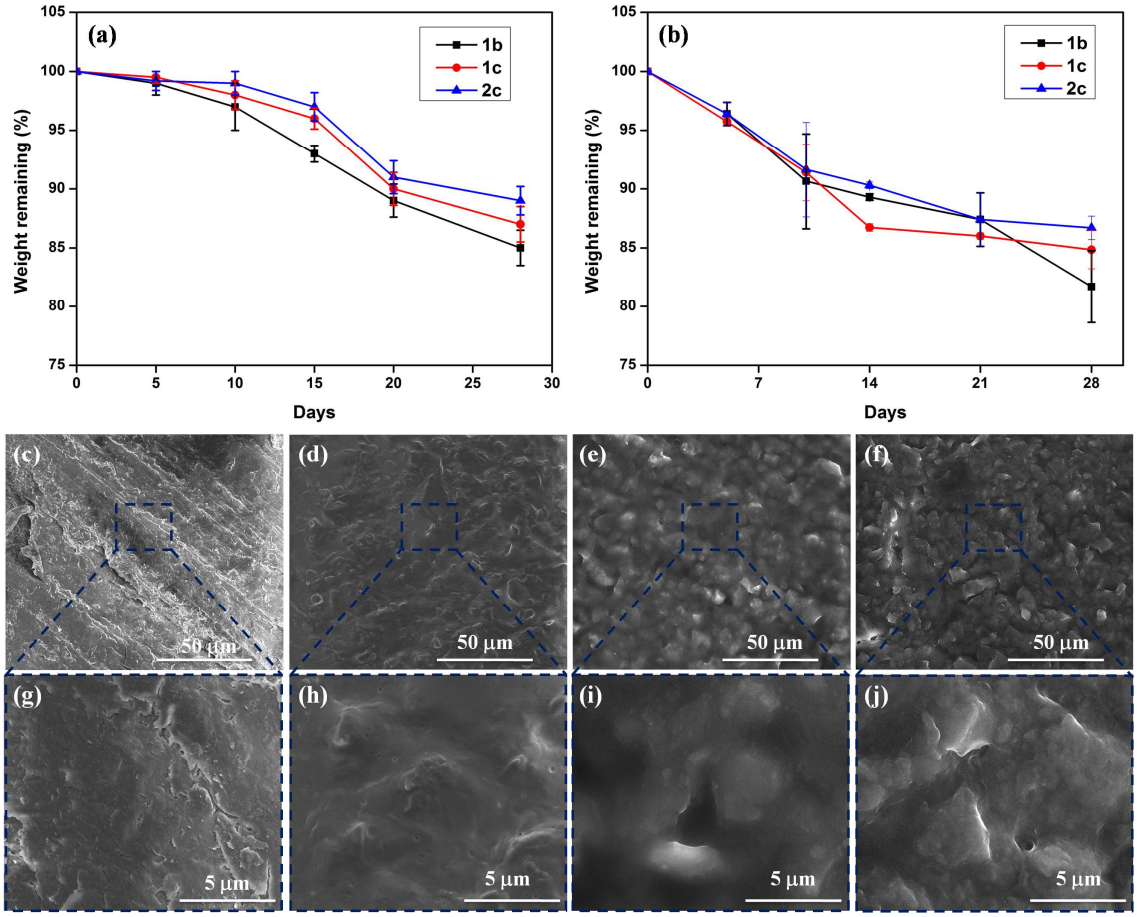

Figure 5. *In vitro* and *in vivo* biodegradation of polymers. (a) *In vitro* degradation in the presence of lysozyme by weight-loss method; (b) *in vivo* degradation upon subcutaneous implantation of disc of polymer in rat by weight-loss method. Scanning electron microscopy images of disc of polymer **2c**: (c and g) surface of the untreated disc; (d and h) surface of the disc after 14 days; (e and i) surface of the disc after 21 days and (F and J) surface of the disc after 28 days. (c-f) Represent low resolution images and (g-j) represent high resolution images respectively.

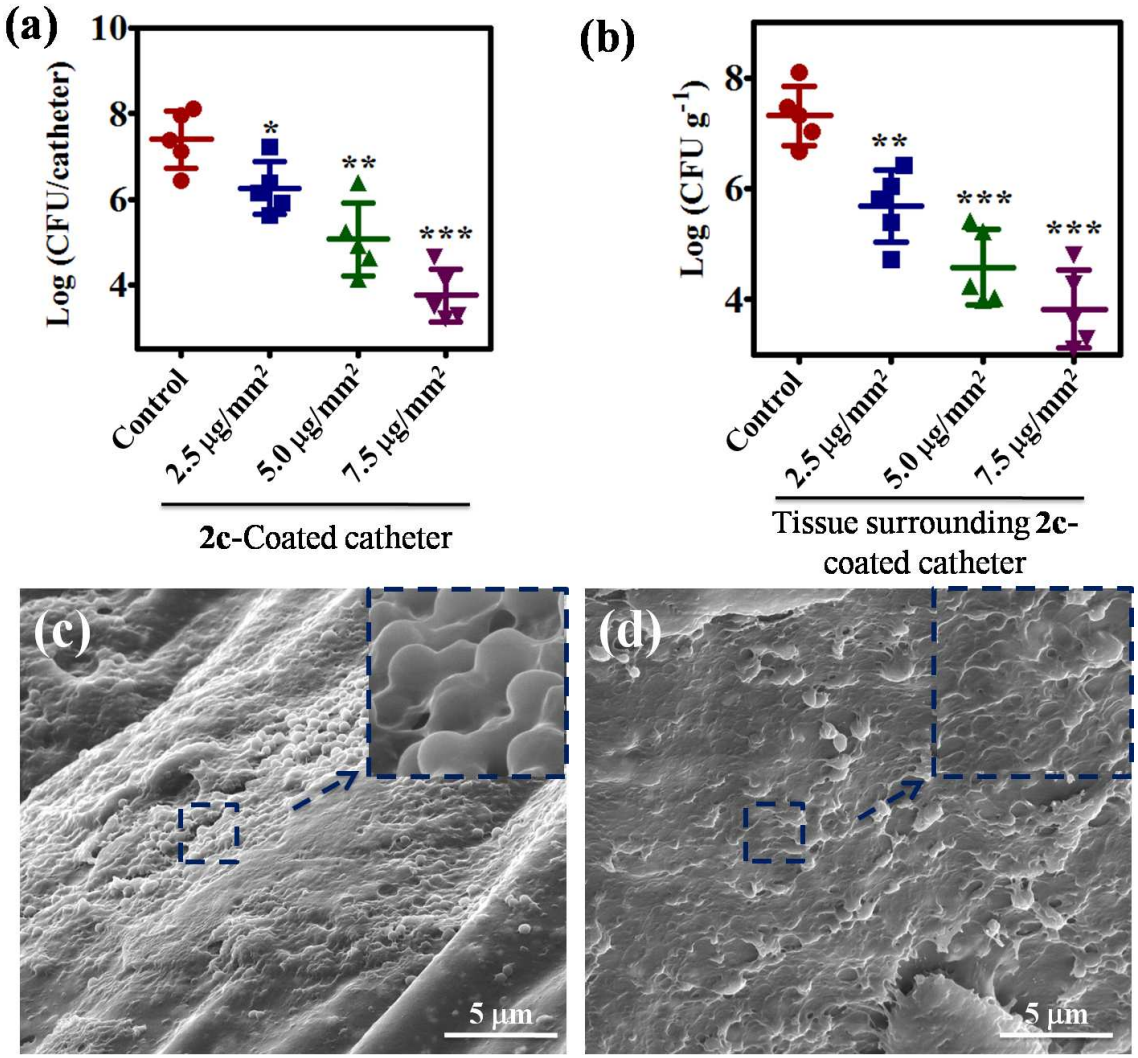

Figure 6. *In vivo* antibacterial activity of polymer-coated catheters. Effect of polymer-coated catheters on methicillin-resistant *S. aureus* (MRSA) inoculated at the time of catheter insertion: (A) bacterial count after harvesting catheter from mice; (B) bacterial count from the catheter surrounding tissue samples. Field emission scanning electron microscopy (FESEM) images of (C) non-coated catheter and (D) **2c**-coated catheter (Inset showing the high resolution microscopy images).

Table 1. Antibacterial and hemolytic activities of polymer coated surfaces

Polymers	MIA (μg/mm^2)						HA_{50} (μg/mm^2)
	Wild type bacteria			Drug resistant bacteria			
	S. aureus	*E. coli*	*P. aeruginosa*	MRSA	VRE	*K. pneumoniae*	
1b	0.12	7.8	7.8	0.62	0.24	7.8	> 31.2
1c	0.12	3.9	15.6	0.32	0.12	7.8	> 31.2
2a	0.48	7.8	31.2	0.78	0.48	31.2	> 31.2
2b	0.24	3.9	15.6	0.39	0.24	15.6	> 31.2
2c	0.06	3.9	7.8	0.06	0.06	15.6	> 31.2
3a	0.24	15.6	31.2	0.32	0.24	> 31.2	> 31.2
3b	0.24	15.6	> 31.2	0.32	0.24	> 31.2	> 31.2
3c	0.12	31.2	> 31.2	0.24	0.32	> 31.2	> 31.2

MRSA = Methicillin-resistant *S. aureus* (ATCC 33591); VRE = vancomycin-resistant *E. faecium* (ATCC 51559); *K. pneumoniae* = beta-lactam-resistant *K. pneumoniae* (ATCC 700603)

Table of Content Graphic

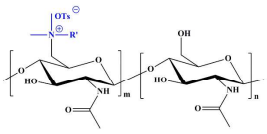

Water insoluble and organo-soluble;
Painted non-covalently onto various surfaces;
Active against drug-sensitive and drug-resistant bacteria

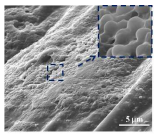

Non-coated medical grade catheter: MRSA contaminated catheter shows the prevalence of bacteria and biofilm formation

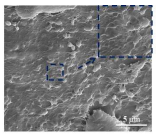

Polymer coated medical grade catheter: MRSA contaminated catheter shows the reduction of bacteria and no biofilm formation